

# Analysis of the temperature influence on Langmuir probe measurements on the basis of gyrofluid simulations

F.P. Gennrich<sup>1</sup>, J. Peer<sup>1</sup>, A. Kendl<sup>1</sup> and B.D. Scott<sup>2</sup>

<sup>1</sup> Institute for Ion Physics and Applied Physics, University of Innsbruck, Association Euratom-ÖAW, Technikerstraße 25, A-6020 Innsbruck, Austria

<sup>2</sup> Max-Planck-Institute for Plasma Physics, Euratom Association, Boltzmannstr. 2, D-85748 Garching, Germany

## Introduction

In the turbulent edge region of magnetically confined plasmas Langmuir probes are frequently used to measure time series of ion saturation current  $I_{\text{is}}$  and floating potential  $V_{\text{fl}}$ . Following the elementary Langmuir probe theory, which assumes a Maxwellian electron velocity distribution and neglects secondary electron emission from the probe, these are related to the fluctuating plasma density  $n = n_{\text{e}} \simeq n_{\text{i}}$  and the plasma potential  $\Phi$  by expressions involving the temperatures  $T_{\text{e}}$  and  $T_{\text{i}}$  ([1], [2]):

$$I_{\text{is}} = A_{\text{i}} e n \sqrt{\frac{k_{\text{B}}(T_{\text{e}} + T_{\text{i}})}{m_{\text{i}}}} \quad (1)$$

$$V_{\text{fl}} = \Phi - \left( \frac{k_{\text{B}} T_{\text{e}}}{e} \right) \ln \left( \frac{I_{\text{es}}}{I_{\text{is}}} \right) = \Phi - \left( \frac{k_{\text{B}} T_{\text{e}}}{e} \right) \ln \left( \frac{A_{\text{e}}}{A_{\text{i}}} \sqrt{\frac{T_{\text{e}}}{T_{\text{e}} + T_{\text{i}}}} \sqrt{\frac{m_{\text{i}}}{2\pi m_{\text{e}}}} \right). \quad (2)$$

$A_{\text{e}}$  and  $A_{\text{i}}$  specify the probe collecting areas for electrons and ions, the electron saturation current is given by  $I_{\text{es}} = A_{\text{e}} e n (1/4) \sqrt{(8k_{\text{B}} T_{\text{e}})/(\pi m_{\text{e}})}$  and  $T_{\text{i}}$  is often assumed to be equal to  $T_{\text{e}}$ . A measurement of the electron temperature with single Langmuir probes requires a sweeping of a preferably complete probe characteristic, which results in a low time resolution. Therefore temperature fluctuations are commonly neglected, albeit there are recent promising results of fast sweeping probes on the one hand [3] as well as developments of more sophisticated probes aiming at a direct measurement of the plasma potential on the other hand ([1], [4]). In order to study the influence and significance of temperature fluctuations on calculations of the plasma parameters from simulated time series of  $I_{\text{is}}$  and  $V_{\text{fl}}$ , the global nonlinear three-dimensional gyrofluid simulation code *GEMR* ([5]–[9]) has been used, which delivers time series of densities, temperatures, and the plasma potential at different radial positions around the separatrix. This allows a direct comparison of synthetically measured quantities and the actual plasma parameters within the simulation.

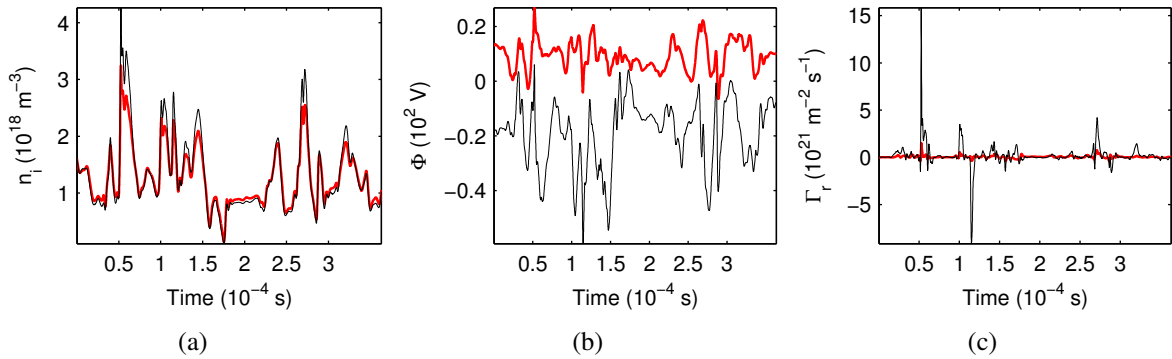


Figure 1: L-mode situation: (a) Time series of code output  $n_i$  (red bold line) and  $n_i^{\text{avg}}$  (black thin line) calculated from  $I_{\text{is}}$  using averaged temperature values. (b)  $\Phi$  (red bold line) and  $V_{\text{fl}}$  (black thin line). (c) Radial particle flux  $\Gamma_r$  calculated from  $\Phi$  and  $n$  (red bold line) and from  $V_{\text{fl}}$  and  $I_{\text{is}}$  (black thin line). The data is collected within the scrape-off layer (GEMR simulation).

## Results

For a first exemplary situation corresponding to an operation in saturated L-mode, the electron dynamical plasma beta is set to  $\beta_e = (\mu_0 p_e)/B^2 \approx 9.4 \cdot 10^{-5}$  and the background mid-pedestal parameters are  $T_e = 150\text{eV}$ ,  $T_i = 180\text{eV}$ ,  $n_e = n_i = 1.25 \cdot 10^{19} \text{m}^{-3}$  and  $B = 2.0\text{T}$ . Major torus radius and aspect ratio conform to ASDEX Upgrade values and for the ion mass  $m_D = 3670m_e$  is used.

As shown in fig. 1(a), the discrepancy between the ion density  $n_i$  and  $n_i^{\text{avg}}$ , the density calculated from  $I_{\text{is}}$  by means of averaged temperature values, is large at points of maxima and minima, but small elsewhere and there is no significant difference in terms of fluctuations. This holds for all positions in the radial simulation domain. In contrast, time series of  $\Phi$  and  $V_{\text{fl}}$  differ considerably (fig. 1(b)). Their difference is given by a product of the electron temperature in energy units, divided by  $e$ , and the dimensionless quantity  $\ln(I_{\text{es}}/I_{\text{is}})$ , which depends on the temperature as well. Both factors are subject to radial variations and strong local temperature fluctuations are mainly responsible for large differences of the fluctuating parts. For experimental estimations of the fluctuation-induced radial particle flux  $\Gamma_r = \tilde{n}\tilde{v}_r$ , the density is usually inferred from  $I_{\text{is}}$  and the radial drift velocity  $\tilde{v}_r$  is considered as radial component of the fluctuating  $\tilde{\mathbf{E}} \times \mathbf{B}$  velocity and computed using potential measurements at two spatially separated positions. However, the instantaneous particle flux calculated from the gradient of the floating potential instead of the plasma potential shows much larger fluctuations than the real flux (fig. 1(c) and 2(b)), which also affects the radial profile of the mean fluxes (fig. 2(a)). This is essentially due to differences in the temperature fluctuations at the respective positions, whereas the use of the temperature averaged density  $n_i^{\text{avg}}$  does not seem to have a decisive impact.

The difference in the fluctuating parts of  $\Phi$  and  $V_{\text{fl}}$  and, consequently, in the corresponding

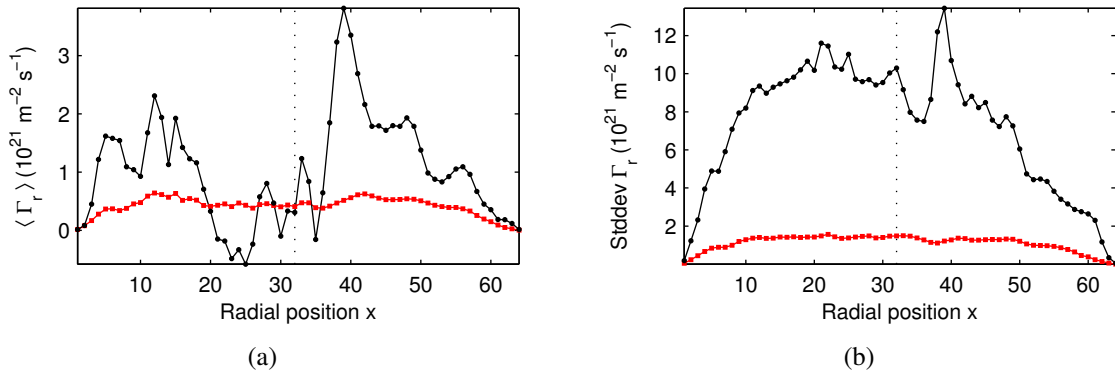


Figure 2: L-mode situation: (a) Radial profiles of the time averaged particle flux  $\langle \Gamma_r \rangle$ , (b) standard deviation  $\text{Stddev}(\Gamma_r)$ . Real values are plotted as red line with squares, values calculated from  $V_{\text{fl}}$  and  $I_{\text{is}}$  as black line with circles.

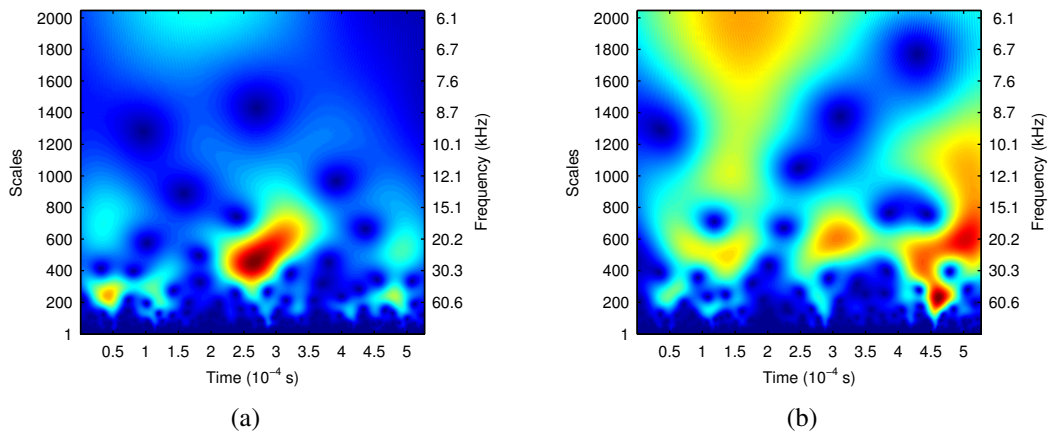


Figure 3: L-mode situation: Wavelet scalogram of (a)  $\tilde{\Phi}$  and (b)  $\tilde{V}_{\text{fl}}$ , collected within the SOL (Morlet Wavelet with cent. frq.  $\omega_0 = 2\pi$  and bandwidth  $\gamma_b = 1$ , modulus of the coefficients).

frequency characteristics is clearly visible in the time-localised Wavelet scalograms (fig. 3). Although the frequency behaviour of  $\Phi$  is largely included in the scalogram of  $V_{\text{fl}}$ , the latter shows numerous additional frequency contributions.

As second case, the investigation has been performed for the gyrofluid simulation of an ELM type-I like ideal ballooning mode situation, exhibiting a large interchange blowout connected with enhanced fluctuations [7]. The simulation parameters are  $T_e = 300 \text{ eV}$ ,  $T_i = 360 \text{ eV}$ ,  $n_e = n_i = 2.5 \cdot 10^{19} \text{ m}^{-3}$  and  $\beta_e \approx 4.0 \cdot 10^{-4}$ . Also in this case, the difference between  $n_i$  and  $n_i^{\text{avg}}$  is relatively small and most distinctive during the large peaks (fig. 4(a)), but there are substantial differences between the fluctuations of  $\Phi$  and  $V_{\text{fl}}$  (fig. 4(b)), in particular near the separatrix and in the SOL, as well as between the real flux and the flux calculated from floating potential and ion saturation current (fig. 4(c)). These are reflected not only in the temporal evolution but also in statistical properties.

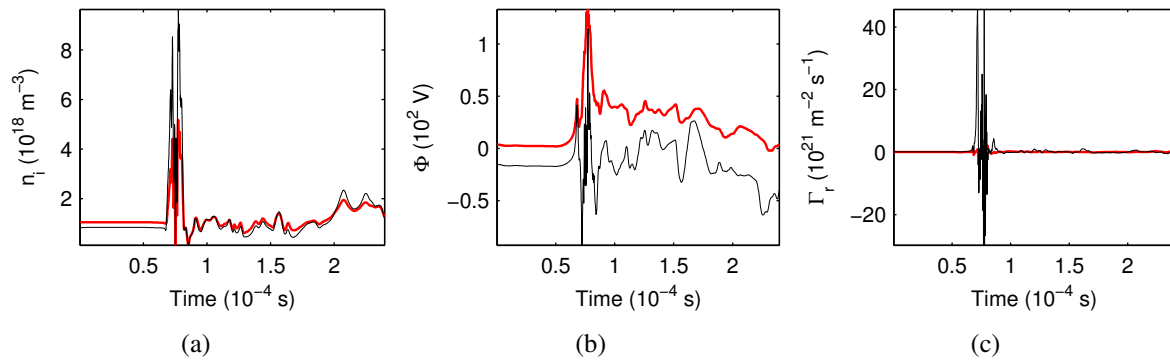


Figure 4: IBM case: (a) Time series of code output  $n_i$  (red bold line) and  $n_i^{\text{avg}}$  (black thin line) calculated from  $I_{\text{is}}$  using averaged temperature values. (b)  $\Phi$  (red bold line) and  $V_{\text{fl}}$  (black thin line). (c) Radial particle flux  $\Gamma_r$  calculated from  $\Phi$  and  $n$  (red bold line) and from  $V_{\text{fl}}$  and  $I_{\text{is}}$  (black thin line). The data is collected within the scrape-off layer (GEMR simulation)

## Acknowledgments

This work was partly supported by the Austrian Science Fund FWF under Contract No. Y398, by the Austrian Ministry of Science BMWF as part of the UniInfrastrukturprogramm of the Forschungsplattform Scientific Computing at LFU Innsbruck, and by the European Communities under the Contract of Associations between Euratom and the Austrian Academy of Sciences, carried out within the framework of the European Fusion Development Agreement. The views and opinions herein do not necessarily reflect those of the European Commission.

## References

- [1] R. Schrittwieser *et al.*, Plasma Phys. Control. Fusion **44**, 567-578 (2002)
- [2] P.C. Stangeby, J. Phys. D: Appl. Phys. **15**, 1007 (1982)
- [3] H.W. Müller, J. Adámek, J. Horacek, C. Ioniță, F. Mehlmann, V. Rohde, R. Schrittwieser and the ASDEX Upgrade Team, Contrib. Plasma Phys. **50**, 847-853 (2010)
- [4] J. Horacek *et al.*, Nucl. Fusion **50**, 105001 (2010)
- [5] B.D. Scott, Contrib. Plasma Phys. **46**, 714-725 (2006)
- [6] B.D. Scott, Phys. Plasmas **12**, 102307 (2005)
- [7] A. Kendl, B.D. Scott and T. Ribeiro, Phys. Plasmas **17**, 072302 (2010)
- [8] T. T. Ribeiro and B. Scott, Plasma Phys. Control. Fusion **47**, 1657-1679 (2005)
- [9] T. T. Ribeiro and B. Scott, Plasma Phys. Control. Fusion **50**, 055007 (2008)